Journal of Applied Sciences

ISSN 1812-5654

science alert

ANSInet
an open access publisher
http://ansinet.com

Journal of Applied Sciences 8 (11): 2091-2097, 2008
ISSN 1812-5654

Experimental Study of Gas Injection Effect as a Secondary Phase on Flow Induced Rotary Hub

N.M. Nouri, A. Sarreshtehdari and E. Maghsoudi
Applied Hydrodynamics Laboratory, Department of Mechanical Engineering,
Iran University of Science and Technology, Narmak 14464, Tehran, Iran

Abstract: Rotational velocity changes, via shear stress modification, due to air bubbles injection in a rotary device experimentally investigated. Air bubbles injected to the water flow crosses the neighbor of the hub which can rotate just by water flow shear stresses. Increasing air void fraction lead to decrease of shear stresses exerted on the hub surface until in high void fractions, the hub motion stopped as observed. Amount of skin friction decrease has been estimated by counting central hub rotations. Wall shear stress decreased as bubbles were injected in the all range of Re changing from 60378 to 61238 and also by increasing air void fraction from 1.22 to 3.06%. Skin friction reduction more than 80% achieved in this study as maximum measured volume of air fraction injected to fluid flow. Remarkable obtained skin friction reduction in this special case indicates the possibility of drag reduction by injection of low amount of air on rotary parts in liquid phase (e.g., water) while this effect is unfavorable in cases where shear stress is a useful phenomena (e.g., mixing).

Key words: Skin friction reduction, air injection, turbulence modification

INTRODUCTION

In recent three decades, using bubbles especially in small sizes (microbubbles) to decrease skin friction has been increased.

In a moving object in an incompressible field, like as water, especially in low Froude numbers more than 80% of drag components are related to skin friction (Kodama *et al*., 2000) but Air-bubbles have been used in various fields such as purification of water quality, promoting the growth of shellfishes, improving physiological activation and some physiochemical properties (Serizawa *et al*., 2003).

McCormick and Bhattacharyya (1973) showed a significant reduction of frictional resistance can be achieved using microbubbles, at low void fractions. In their work, hydrogen microbubbles generated by electrolysis produced up to 30% drag reduction over a body of revolution with less than 1% void fraction. They also showed that as the Reynolds number of the liquid increased, the effectiveness of microbubbles in reducing drag diminished with the same gas injection rate. Moreover, the drag reduction degree of persistence was greater at lower speeds with a given gas injection rate and the drag reduction increased with the increase of gas injection rate. Microbubbles have been shown the capability of achieving drag reductions as high as 80% on flat plate boundary layers as in polymer drag reduction (Madavan *et al*., 1984, 1985a, b). By combining polymers and microbubbles, Fontaine *et al*. (1999) achieved drag reductions greater than 80%. They suggested that polymer drag reduction was independent of the mechanism responsible for the microbubble skin friction reduction.

There is no complete agreement, despite many studies on microbubble drag reduction, on the microbubble physical phenomenaleading to drag reduction. Issues such as microbubble size and distribution in the boundary layer have been recognized as key parameters in achieving important gains in drag reduction, but the role of such parameters is not yet fully understood. Microbubble generation is another important issue, since the net energy saving in a system must account for the energy required to produce the microbubbles.

Among the main factors considered responsible for the microbubble drag reduction phenomena are the decrease of density, the increase of effective viscosity and the liquid turbulence microbubble interactions. Buoyancy effects in microbubble drag reduction have been reported by Madavan *et al*. (1984). In a flat plate boundary layer, Madavan *et al*. (1985a) achieved higher

Corresponding Author: Ali Sarreshtehdari, Applied Hydrodynamics Laboratory, Department of Mechanical Engineering, Iran University of Science and Technology, Narmak 14464, Tehran, Iran
Tel: +98 912 33 66 793 Fax: +98 21 77240488

drag reduction in their plate-on-top experiment than in the plate-on-bottom case. Sanders *et al.* (2003) reached almost 100% drag reduction when the injected gas formed a layer underneath the flat plate.

Numerical simulations have been used also as a means to investigate the underlying mechanism of microbubble drag reduction. Madavan *et al.* (1985b) determined that microbubble size and distribution in the boundary layer were major issues in the microbubble drag reduction phenomena. Similar results were found by Xu *et al.* (2002) with a Direct Numerical Simulation (DNS) of a fully developed turbulent channel flow using a Force-Coupling Method (FCM). Their results indicate that the initial seeding of microbubbles has an important effect on the pressure gradient and viscous drag force. Furthermore, smaller microbubbles gave a sustained reduction in drag, while larger bubbles only exhibited transient drag reduction. A reduction in mean drag of 6.2% was achieved at a void fraction of 4.24%. The microbubbles were seeded from a location having a distance from the wall of y+=20. They obtained a maximum drag reduction of 20.2% at a void fraction of 2%. They concluded that the drag reduction was caused by a velocity divergence effect, associated with the void fraction. The presence of microbubbles generates a local positive divergence of the fluid velocity, creating a positive mean normal velocity at a farther distance from the wall. This reduces the mean streamwise velocity and displaces the quasistreamwise longitudinal vortical structures away from the wall due to the presence of bubbles. This displacement increases the spanwise gaps between the wall streaks associated with the sweep events and reduces the streamwise velocity of these streaks.

Although DNS of microbubble turbulent boundary layers provides insight into the physical phenomena responsible for the drag reduction, it is not currently feasible to use it for practical designs of maritime and other transportation means that could take advantage of the drag reduction phenomenon. Thus, multiphase Reynolds Averaged Navier-Stokes (RANS) methods are being developed for simulations of three-dimensional geometries at relevant high Reynolds numbers (Kunz *et al.*, 2007).

In this study, the effect of air bubble injection on skin friction has been investigated experimentally. Rotational behavior of central hub, with complex geometry, was obtained to find operation of device in various void fractions for favorable designed regimes. The device generating bubbles with the size of smaller than 500 μm was used (Nouri *et al.*, 2007). The variation of skin friction by bubbles injection in various void fractions was investigated on the rotational hub of the microbubble generator and rotational velocity of the hub was considered as an effective parameter related straightly to skin friction and changes in flow field. According to the results, skin friction reduction more than 80% was achieved.

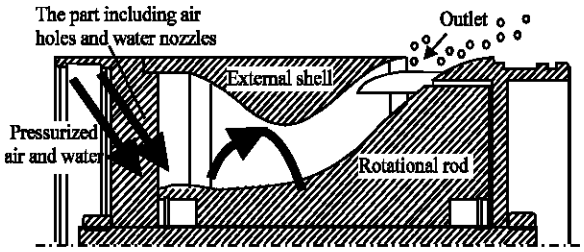

Fig. 1: Section of improved Micro bubble generator device

MATERIALS AND METHODS

The apparatus used for bubble generation is a symmetric cylindrical device including a central rotational hub and an external shell with the height of 160 mm, maximum diameter of 217 mm and thickness of 8.8 mm. Figure 1 shows a section of the device.

In the model, water enters the device via six diagonal nozzles with diameter of 10 mm and angle of 61° and mixes with air coming from 24 vertical straight holes with diameter of 2 mm at the bottom of the device. Passing a rotational trace around central rotational hub, air particles are broken up to tiny bubbles. In the other word, fluid and gas are injected between shell and hub through diagonal and vertical holes, respectively and exit circumferentially through outlet. Bubbles are broken in three different stages in this device. At first stage, they are broken due to the injection trough holes. During the second stage, rotational flow makes bubbles to pass a longer path. In this stage, high velocity flow increases separation between bubbles, reducing coalescence and turb-ulent flow breaks them continuously. In the last stage, large shear stresses caused by narrow outlet break the bubbles for the last time.

Geometrical shape of the region through which liquid-gas mixture passes is deliberately selected to maximize rotational velocity of gas-fluid mixture. Angles of diagonal holes of water are selected so that the tangential velocity of inlet water is much more than radial velocity in order to make central hub rotate (Fig. 2).

Two bearings have been used to support the central hub and promote the tendency of rotation. In order to obtain an optimum geometry for the area that liquid-gas

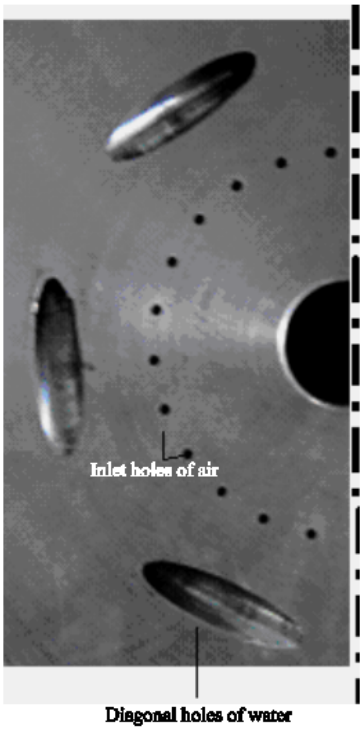

Fig. 2: Straight and diagonal holes trough which air and water injected to the system

mixture passes, finite element method was used to simulate single phase flow for four different geometries proposed during design procedure. Rotational velocity in the region, Turbulent Kinetic Energy and the trajectories at which water elements travel were considered as the effective parameters for optimum geometry selection (Nouri *et al*., 2007).

The More Turbulent Kinetic Energy and the longer the trajectories of water elements, the less the size of generated bubbles would be. Manufacturability of the geometry was another considered issue.

The final model device was designed according to the numerical results, base on the maximum Turbulent Kinetic Energy, rotational velocity and length of trajectories of water elements.

In single phase flow and computer simulations integrated force can be computed using shear stress, therefore effective torque yielded (Eq. 1):

$$T = 2\pi\int \tau r^2(h)\,dh \qquad (1)$$

where, T is torque, r, h are radius and height of hub and τ is shear stress. It is pointed out that only the component of the wall shear stress vector in planes perpendicular to the axis of the hub affects the rotational forces acting on the hub. The other component of the wall shear stress, the

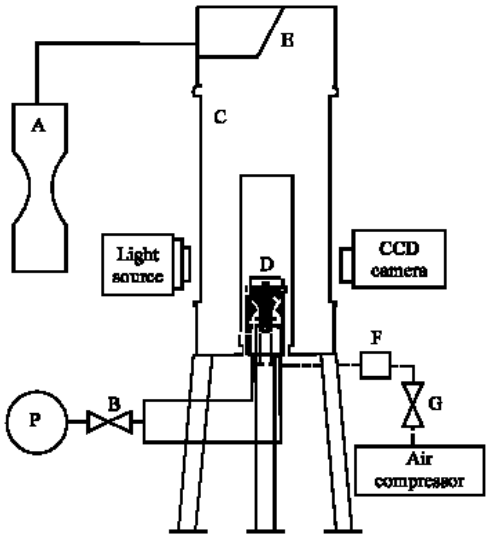

Fig. 3: Experiment set-up of Improved Microbubble Generator Device (A: Water flowmeter, B: Water flow control valve, C: Experiment tank, D: The device, E: Membrane, P: Pump, F: The rotameter, G: Air flow control valve)

component with a vector lying in planes that extend through the axis of the hub, does not directly affect the rotation of the hub. Therefore as a consequence, the measured hub rotation rate can only be used to infer how this one component of the skin friction force was affected by gas injection.

Figure 3 shows the experimental set-up. Microbubble Generator was installed at the bottom of a cylindrical tank with depth of 1.5 m and volume of 1.57 m^3. The tank has four trans-parent windows for setting light and taking images. Each two windows are exactly designed to be opposite. The first two windows have the height of 1 m and width of 0.3 m and are set near the bottom of the tank. The second two windows with the height of 1.2 m and width of 0.3 m are set 0.5 m upper than the bottom of the tank. Since the second two windows are cover the region located exactly after outlet of two windows are cover the region located exactly after outlet of the apparatus, these ones were used for film-taking and photography. Water is entered the water nozzles via a centrifugal pump (p). Flow rate is measured by a flow meter and is controlled using a valve (B). A compressor with maximum pressure of 500 kPa is used to provide and inject pressurized air, after passing through a pressure regulator, to straight air holes of the device. Before air enters the device, its flow rate is measured by a calibrated rotameter (F) and controlled by a valve (G). The pressure of injected air was adjusted to 110±5 kPa in all experiments.

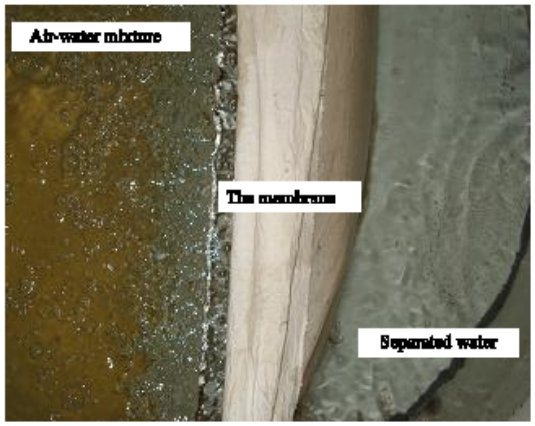

Fig. 4: Membrane which was used to separate water from bubbles

Some qualitative tests show that bubbles are located close enough to the hub to affect on skin friction in this device. Bubbles leaving the apparatus gradually coalesced as they rose and made large bubbles. So, at the top of the tank, a membrane (E) was used to separate air from water in order that inlet water feeding to the flow meter and the pump was free of air bubbles (Fig. 4).

Maximum roughness of Central hub, with an effective diameter of 132 mm, was estimated to 0.003. Hence, tangential component of shear stress between water flow and hub external surface was the only excitation force which made the hub rotation.

Shen *et al*. (2006) showed that water impurities, like as salt and other surfactant solution can affect on micro bubble size distribution and skin friction changes consequently, therefore in these tests purity of water is constant in all of test steps.

To investigate bubble injection effect on skin friction, two series of test was conducted. At first, air injection or air flow rates were fixed and water flow rate was decreased in eight steps. Then, at the second series, the last water flow rates were fixed and air flow rate increased in each step.

In each step, the hub was film-taken by a digital CCD camera, Sony DSC W30, with ability of 30 fps, movie resolution of 640*480 pixels and with sensitivity of ISO 1000. Since the maximum rotational velocity of hub was under 200 rpm, using this camera seems logical. Duration time of each film-taking took between 30 and 60 sec depending on the rotational velocity of the hub. The time was longer for the tests in which the rotational velocity was less than the others. In addition, a gap time around 60 sec existed between each two consequent test in order that all parameters such as air flow rate and water flow rate were stable and constant.

A reflector on the hub allowed the rotational speed to be measured from the camera data. During film-taking, flow rates of water and air were recorded in order to calculate void factions of each test. Since the time between each two observations of the reflector was definite, the rotational velocity in each experiment was easily determined. In these experiments, relative error of rotational velocity is less than 0.01.

RESULTS AND DISCUSSION

All the tests were carried out in turbulent flow with a volumetric water flow rates changing from 0.0047 to 0.0048 (m^3 sec^{-1}), to achieve various Reynolds numbers. The apparatus adjustments confined water flow rates in above range. The data of the Reynolds numbers changing from 60378 to 61238 calculated based on diameter of the pipe feeding the apparatus, the bulk velocity estimated by ventury meter and the viscosity of water. Also, the rate of air injected to flow was changed from 0 to 0.00015 (m^3 sec^{-1}) in order to find out the effect of void fraction variations on skin friction.

The void fraction inside the apparatus gap was not controlled but the gas flow rate was measured by a gas flow meter. The average void fraction in the test section is estimated by, (Eq. 2):

$$\alpha = \frac{Q_a}{Q_w + Q_a} \quad (2)$$

where, Q_a and Q_w are air flow rate and water flow rate, respectively. The uncertainty of air flow rate is 0.001 according to air flow meter and that of water flow rate is 0.1 in relative error. Therefore, the measurement uncertainty of the average void fraction is 10-2.

Compressed air with back pressure of approximately 110 kPa which entered to the bottom of the apparatus leaded to create bubbles by small sizes while water flow circulates in the setup. Above mentioned water and air flow rates were controlled by two valves after flow meters and make void fraction changed from 0 to 3.06%.

Small bubbles with size of smaller than 500 micron in diameter were produced either in minimum or maximum air flow rates as shown in Fig. 5. Bubbles' sizes were determined using image processing method as describing in the former study (Nouri *et al*., 2007).

Increasing void fraction more than about 4% caused two problems preventing high void fractions in experiments in this setup. First, the volume of the produced bubble was increased so that it hided the reflection signs behind the bulky bubble clouds and disallowed surface of the hub to be observed and

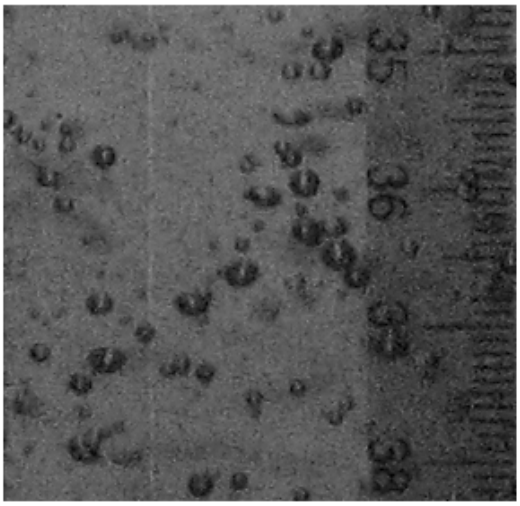

Fig. 5: A sample of produced microbubbles by the apparatus

photographed. Hence, the rotational velocity of hub was not able to be calculated by image processing. Secondly, in this special setup and in void fractions of lower than 10%, the hub stopped completely. This subject was investigated by increasing void fractions more than 4% in each test and reducing it suddenly. Stationary hub was observed in all repeated tests as above procedure for the void fractions changing from 4 to 10%.

Figure 6 shown hub rotational velocity based on water flow rates changes, in various air injection rates. This figure illustrates that by increasing water flow rates, in each air injection rate, the rotational velocity raise up and vise versa. In this figure, the approximately parallel lines, in a constant air flow rate, indicates the similar rotational behavior in single and two phase flow, although it is important to consider that the slope of each line changes and decreases by increasing the air flow rates. In the other word, not only hub rotational velocity but also its variation versus water flow rate is decreased by increasing air flow rate. A linear trend line based on least square method among experimental data gives an absolute slope bond changing from 2.41 to 1.10 for single phase flow and air injection of 0.1494 L sec^{-1}, respectively.

Figure 7 presents the results of hub rotational velocity changes in the constant water flow rates by increasing air flow injection rates. As shown in the Fig. 7, rotational velocity is obviously decreased by increasing air injection or void fraction. By dividing rotational velocity of each water flow rate to its maximum value in single phase condition, Relative Rotational Velocity (RRV) was extracted which is one of the operating characteristics of this apparatus (Eq. 3).

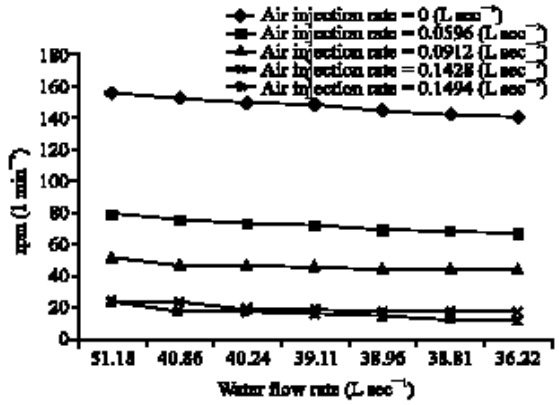

Fig. 6: Velocity changes by decreasing water flow rate in various air injecting rates

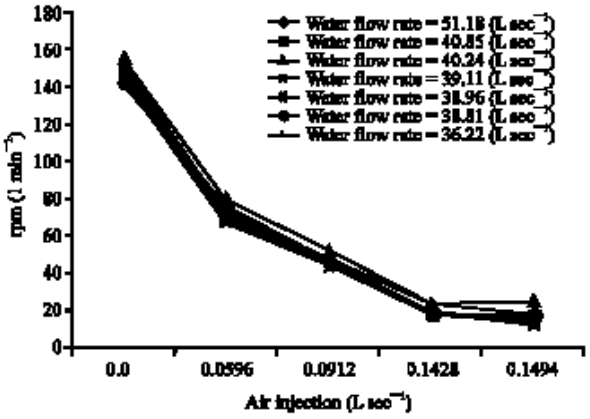

Fig. 7: Velocity changes by increasing air flow rate in various water flow rates

$$RRV = \frac{\omega}{\omega_0} \quad (3)$$

A series of repetitive tests were conducted to investigate RRV changes in constant void fractions. The results of these tests indicate a normal distribution with mean values and standard deviations shown in Table 1. A sample of these tests presented in Fig. 8.

Figure 9 indicates relative rotational velocity versus void fraction. In this figure, mean values of RRVs were extracted from Table 1 and the errors bars show deviations of mean values. By considering this amount based on Student-t-test, all of data with the probability of more than 95% will coincide with mentioned bound.

The amount of RRV is decreased by increasing void fraction as shown in Fig. 9. Since number of rotations of hub is a significant parameter for the apparatus operation (microbubble generating), this figure can be used as an anticipator of rotational velocity of hub shown as a trend

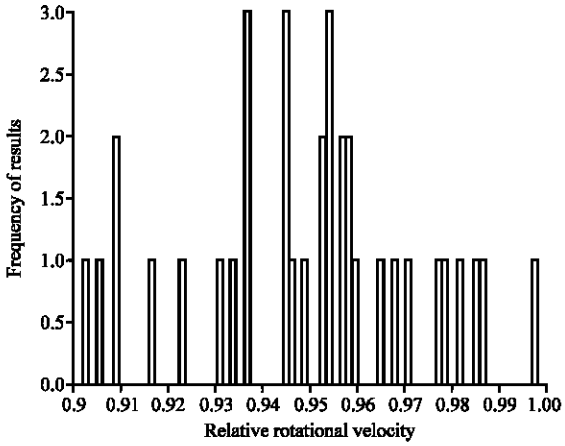

Fig. 8: Relative rotational velocity repetitive tests histogram

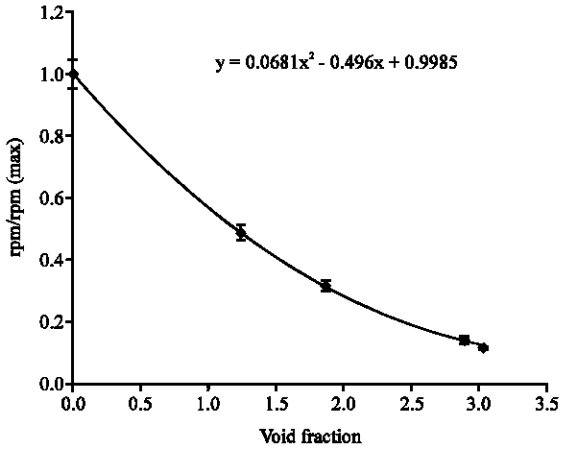

Fig. 9: Relative rotational velocity by void fraction changes

Table 1: Test results normal distribution

	Void fractions (%)				
Statistics	0	1.23	1.88	2.92	3.05
Mean values	1	0.460	0.300	0.130	0.110
Standard deviations	0	0.025	0.015	0.016	0.025

Table 2: Skin friction reduction (%)

	Void fraction (%)				
Reynolds No.	0	1.22	1.86	2.89	3.06
61238	-	52.00	68.00	84.00	88.00
60595	-	54.08	69.39	86.73	90.82
60487	-	55.10	70.41	87.76	90.82
60378	-	53.68	69.47	87.37	91.58
Average	-	53.72	69.32	86.46	90.30

line by a polynomial of second order. The amount of C_f and C_{f0} can be obtained easily if shear stress is assumed to change by rotational velocity linearly. So, the percentage of skin friction reduction (SR) was determined via following equation (Eq. 4):

$$SR = 1 - \frac{C_f}{C_{f0}} \quad (4)$$

Table 2 presents the percent of skin friction reduction in each Reynolds number. Each row includes the relative skin friction reductions in comparison with single phase condition of the same Re number. Results in this case, indicate small percentage of air void fraction, less than 5%, maybe cause strong effect on flow induced motion resulted by skin friction. In this case, this table indicates small percentage of air void fraction, less than 5%, maybe cause strong effect on flow induced motion resulted by skin friction.

CONCLUSIONS

An experimental study on a rotational hub which used in a flow mixing device was conducted to investigate the effect of air bubble injection on the skin friction reduction and device operation consequently. In this setup water flow tangential jets prepare rotational motion of hub due to skin friction between fluid flow and external surface of rotational hub. In this study, rotational velocity of central apparatus' hub was considered as a sign of skin friction and its changes were investigated. The following results have been obtained:

In this special case, the tangential water jets caused skin friction on the external surface of hub and rotated it by constant velocity. So, increasing of water flow rate in each void fraction lead to increasing velocity and vise versa.

In this setup, the same behavior of rotational velocity was obtained either by changing water flow rates in constant air flow injections or by changing air flow injection in constant water flow rates. On the other hand, when air flow rate was set constant but water flow rate was changed not only hub rotational velocity but also its variation versus water flow rate was decreased by increasing air flow rate.

In this case, small values of void fraction significantly affected on skin friction which creates rotational velocity. Obtained results indicated that void fractions less than 4 percent caused around 90 percent decrease of skin friction in this special setup.

This method (MBDR) can be used to avoid skin friction resistant forces, affecting on Rotating parts of machines.

Bubbles size and distribution, kind of injected gas and background flow properties are so vital parameters affecting skin friction that have been proposed for next steps of this study.

ACKNOWLEDGMENTS

The Research has been financed by Applied Hydrodynamics Laboratory of Mechanical Engineering Department, Iran University of Science and Technology. The authors would like to thank Applied Hydrodynamics Laboratory for facilities and fund and also express their appreciation to Mr. Allahyari and Mr. Arabshahi for experimental assistance.

REFERENCES

Fontaine, A., S. Deutsch, T.A. Brungart, H.L. Petrie and M. Fenstermacker, 1999. Drag reduction by coupled systems: Microbubble injection with homogeneous polymer and surfactant solutions. Exp. Fluids, 26 (5): 397-403.

Kodama, Y., A. Kakugawa, T. Takahashi and H. Kawashima, 2000. Experimental study on microbubbles and their applicability to ship for skin friction reduction. Int. J. Heat Fluid Flow, 21 (1): 582-588.

Kunz, R.F., H.J. Gibeling, M.R. Maxey, G. Tryggvason, A. Fontaine, H. Petrie and S.L. Ceccio, 2007. Validation of two-fluid eulerian CFD modeling for microbubble drag reduction across a wide range of Reynolds numbers. Trans. ASME., 129 (1): 66-79.

Madavan, N.K., S. Deutsch and C.L. Merkle, 1984. Reduction of turbulent skin friction by microbubbles. Phys. Fluids, 27 (2): 356-363.

Madavan, N.K., S. Deutsch and C.L. Merkle, 1985a. Measurements of local skin friction in a Reynolds bubble-modified turbulent boundary layer. J. Fluid Mech., 156 (1): 237-256.

Madavan, N.K., C.L. Merkle and S. Deutsch, 1985b. Numerical investigations into the mechanisms of microbubble drag reduction. ASME. J. Fluids Eng., 107 (33): 370-377.

McCormick, M.E. and R. Bhattacharyya, 1973. Drag reduction on a submersible hull by electrolysis. Nav. Eng. J., 85 (1): 11-16.

Nouri, N.M., E. Maghsoudi, A. Sarreshtehdari and M. Yahyaei, 2007. Microbubble generation using high turbulent intensity flow. Proceedings of FEDSM2007. 5th Joint ASME/JSME Fluids Engineering Conference, San Diego, California, USA.

Sanders, W.C., E. Winkel, D.R. Dowling, M. Perlin and S.L. Ceccio, 2003. Bubble friction drag reduction in a high-reynolds-number flat-plate turbulent boundary layer. J. Fluid Mech., 552: 353-380.

Serizawa, A., T. Inui, T. Yahiro and Z. Kawara, 2003. Laminarization of micro-bubble containing milky bubbly flow in a pipe. 3rd European-Japanese Two-Phase Flow Group Meeting, Certosa di Pontignano, 1: 21-27.

Shen, X., S.L. Ceccio and M. Perlin, 2006. Influence of bubble size on micro-bubble drag reduction. Exp. Fluids, 41 (3): 415-424.

Xu, J., M.R. Maxey and G. Karniadakis, 2002. Numerical simulation of turbulent drag reduction using micro-bubbles. J. Fluid Mech., 468 (1): 271-281.